Cell Reports, Volume *25*

Supplemental Information

Brief Local Application of Progesterone via a Wearable Bioreactor Induces Long-Term Regenerative Response in Adult *Xenopus* Hindlimb

Celia Herrera-Rincon, Annie S. Golding, Kristine M. Moran, Christina Harrison, Christopher J. Martyniuk, Justin A. Guay, Julia Zaltsman, Hayley Carabello, David L. Kaplan, and Michael Levin

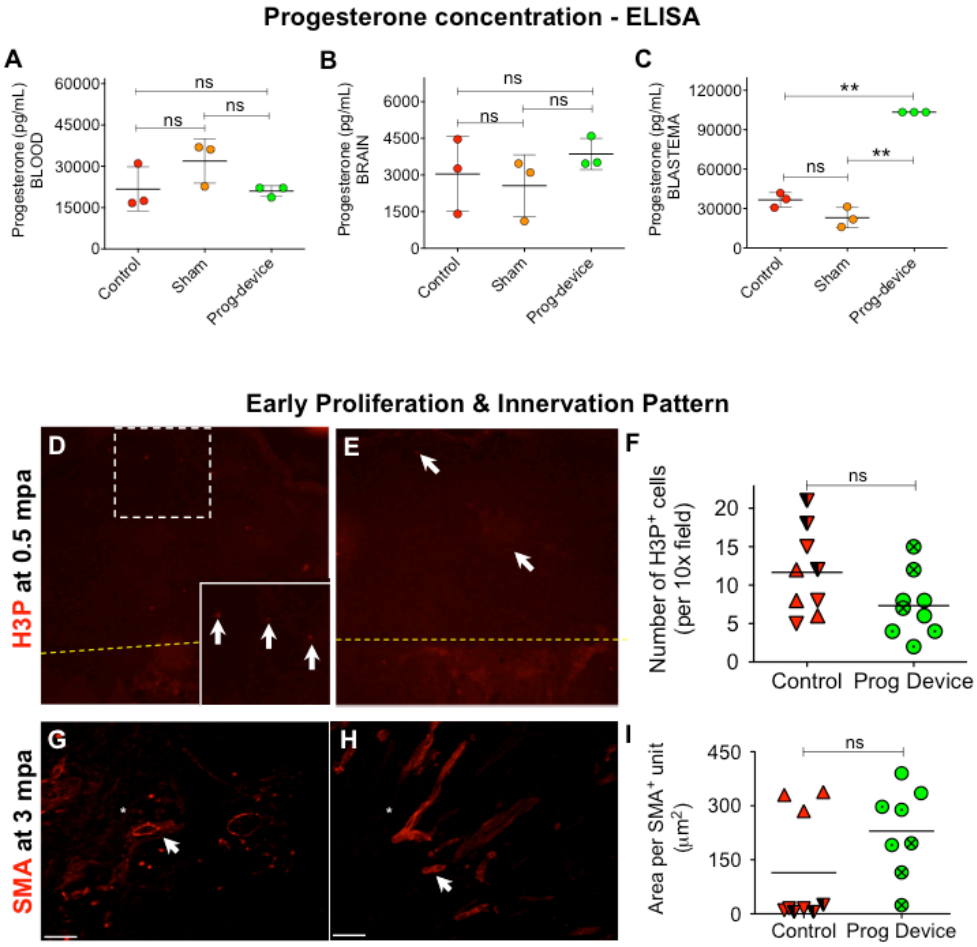

Supplementary Fig. S1. Early response to device attachment: Progesterone levels and proliferation & innervation patterns, Related to Figure 1.

A-C. Progesterone levels in the three experimental groups 24 hours after amputation and device attachment, measured via ELIA both at remote tissues (A&B, blood and brain) and at injury site (C, blastema). Control (untreated after amputation), Sham (only-device treated after amputation) and Prog-device (combined progesterone-loaded device treated after amputation) animals are represented in red, orange and green, respectively. Values are represented with scatter plots, where each dot represents the average value of three biological replicates (n=6 animals per replicate and experimental group). Horizontal lines indicate mean ± sd. *P* values after Bonferroni's post-hoc test (One-way ANOVA $P > 0.05$ for A&B, and $P < 0.01$ for C) are indicated as ** $P < 0.01$, ns: no significant difference. **D-F**. Cell proliferation (after H3P immunofluorescence) in the early fibroblastema (0.5 mpa) of untreated Control (D) and treated Prog-device (E) animals. At this stage, the proliferative response after amputation is weakly starting and no significant differences in the number of H3P-positive cells were detected between groups. In D, the bottom-right insert corresponds to the dashed-white line. Amputation plane is indicated with an orange-dashed line. **G-I.** The presence of organized blood vessels, following the longitudinal axis, was a landmark for Prog-device late blastemas (3 mpa; white asterisk in H compared to G), although not significant differences were obtained after group comparisons.

Scale bar = 100 μm. G,H: Amputation plane is left, lateral is up. F, I: Values are represented with scatter plots, where each dot represents one histological section, and each dot style represents one animal. Horizontal line indicates mean. *P* values after *t*-test are indicated as ns: no significant difference.

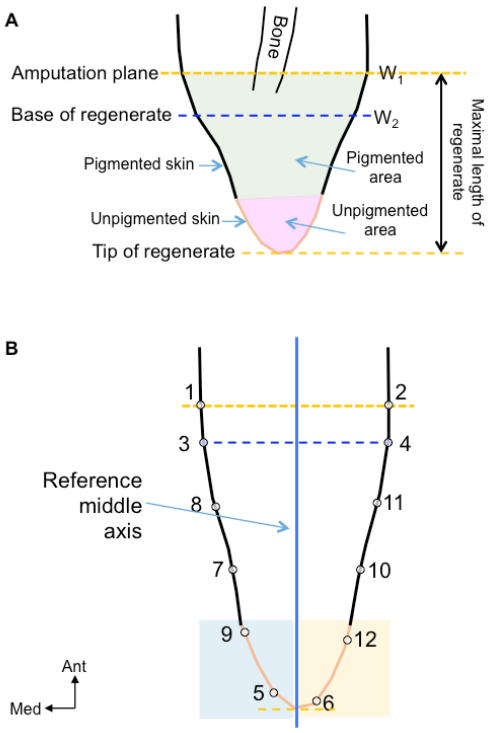

Supplementary Fig. S2. Assessment of the regenerated soft tissue, Related to STAR Methods and Figure 2.

A. Diagram of a prototypical 2-mpa regenerate showing the biological meaningful elements and morphometric parameters used to evaluate the limb outcome over time: percentage of width change (W_2 respect to W_1; WID), percentage of unpigmented area (respect to the total regenerated area; UNA), and maximal length of the regenerate (LEN). WID: Before amputation, the limb has a constant width. This situation is not maintained after amputation and tissues start to narrow while outgrowth is progressing. A lower percentage of width change is, hence, an indicative of regenerative ability, as regenerate is closer to the original morphology, previous amputation. We evaluate the decrease in width experienced by the limb as consequence of the amputation by means of the percentage of change between two width values, before (W_1, width at amputation plane, orange-dashed line) and after (W_2, width at the base of the regenerate, blue-dashed line) amputation, with the formula WID = $(W_2\text{-}W_1)*100/W_1$. UNA: This variable quantifies the differences in pigmentation pattern of the regenerate, by means of the percentage of total regenerated area that is covered by unpigmented epidermis. To this, firstly, we calculated the total area regenerated (from the amputation plane to the tip of regenerate; green and pink surfaces in diagram, respectively). Secondly, a straight line indicating the demarcation of the totally unpigmented portion from the rest of the limb was drawn. Then, the area of the regenerate under that line (unpigmented area) was divided by the total area, with the formula UNA = pigmented area/ (pigmented+ unpigmented area)*100. LEN: We evaluate the maximal length of the regenerate by calculating the distance from the amputation plane to the plane set by the tip of the regenerate (distance between the two orange-dashed lines). To avoid size noise, this value was normalized to the total animal length (or distance from snout to vent, TOT LEN). This morphometric analysis

was performed on regenerates belonging each experimental group (Control and Prog-device, respectively) at five selected times for a 9.5-month period: 0.5, 1, 2.5, 5, 7.5 and 9.5 months post amputation (mpa). Representative images and graphs are indicated in Fig. 2A, B. **B**. Diagram of a prototypical 7.5-mpa regenerate including the positions of the twelve landmarks used for the geometric morphometrics analysis. To describe and quantify the changes in shape of the regenerate between Control and Prog-device groups, we employed MorphoJ software (Klingenberg, 2011), as extensively detailed in (Mondia et al., 2011). MorphoJ performs a geometric morphometric analysis based on landmarks or points used to define the profile of a shape. For our analysis, twelve landmarks defined each regenerate profile: the first six landmarks were biologically meaningful positions: 1 and 2 define the amputation plane, 3 and 4 for the base of the regenerate, 5 and 6 define the points at the tip of the regenerate. The other six points were semi-landmarks, chosen by successively finding the midpoints between the previous positions, as indicated by the numbers in the diagram. Landmarks were placed on digital images using ImageJ. MorphoJ is freely available from http://www.flywings.org.uk/MorphoJ_page.htm. A reference axis, passing through the middle point of a straight line linking landmarks 1 and 2, was placed on each profile. This axis was used to evaluate the curvature at the tip of the regenerate. This parameter was included as criterion for the regeneration Index. Curvature was considered *positive* when the four most distal landmarks (9, 12, 5 and 6) were situated on the same lateral plane (right or left) respect to the middle axis. In this example diagram, 9 and 5 are on left plane (blue square), as 12 and 6 are on the right one (orange square). The tip morphology of the illustrative diagram would be considered *negative* for the variable curvature.

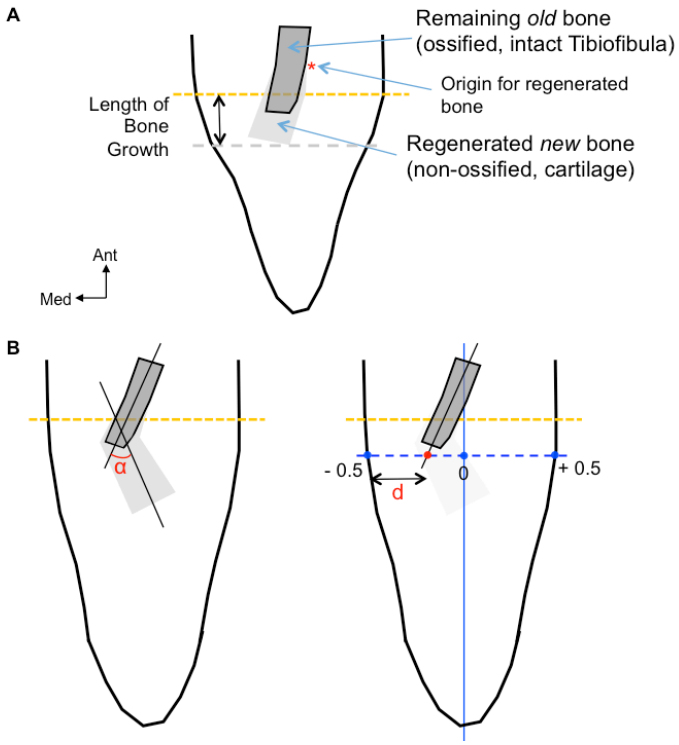

Supplementary Fig. S3. Assessment of the bone growth and its reintegration with the remaining tissues, Related to STAR Methods and Figure 2C.

A. Diagram of a prototypical 2-mpa regenerate, under X-ray image, showing the biological meaningful elements and morphometric parameters used to evaluate the skeletal outcome over time: maximal length of bone from the amputation plane (BLEN; Table 1) and maximal area occupied by *new* bone growth (mostly non-ossified bone or regenerated cartilage, BAREA; Table 1). Responsive animals generated the same bone growth pattern as displayed in the graphic. The skeletal regrowth origin began above the plane of amputation, indicating the occurrence of a secondary or spontaneous amputation (as described in mice by Muneoka's group (Fernando et al., 2011)). The secondary amputation acts as a catalyst for bone regeneration as it creates more bone resorption and degradation. The newly formed bone typically widened at its distal end and deviated from the midline of the intact tibiofibula. The morphometric analysis was performed on regenerates belonging each experimental group (Control and Prog-device, respectively) at five selected times for a 9.5-month period: 0.5, 1, 2.5, 5, 7.5 and 9.5 months post amputation (mpa). Representative images and graphs are indicated in Fig. 3 and Supplementary Fig. S4. **B.** Diagram of a prototypical 7.5-mpa regenerate, under X-ray image, including the axis used to evaluate the reintegration of the regenerated bone and remaining tissues during limb regeneration. Left, Reintegration of the regenerated new bone and the remaining old bone. We evaluated the deviation angle (α) formed under the intersection between the middle line of the new bone growth and the middle line of the remaining bone (longitudinal axis of the tibiofibula). Right, The geometric intersection between the middle line of the intact tibiofibula bone and the plane set by the base of the regenerate was taken for evaluating the old-bone displacement (d) over the course of the

regeneration, from the longitudinal axis to the medial edge of the soft tissue. This morphometric analysis was performed on regenerates belonging each experimental group (Control and Prog-device, respectively). Representative images and graphs are indicated in Fig. 2C-2E.

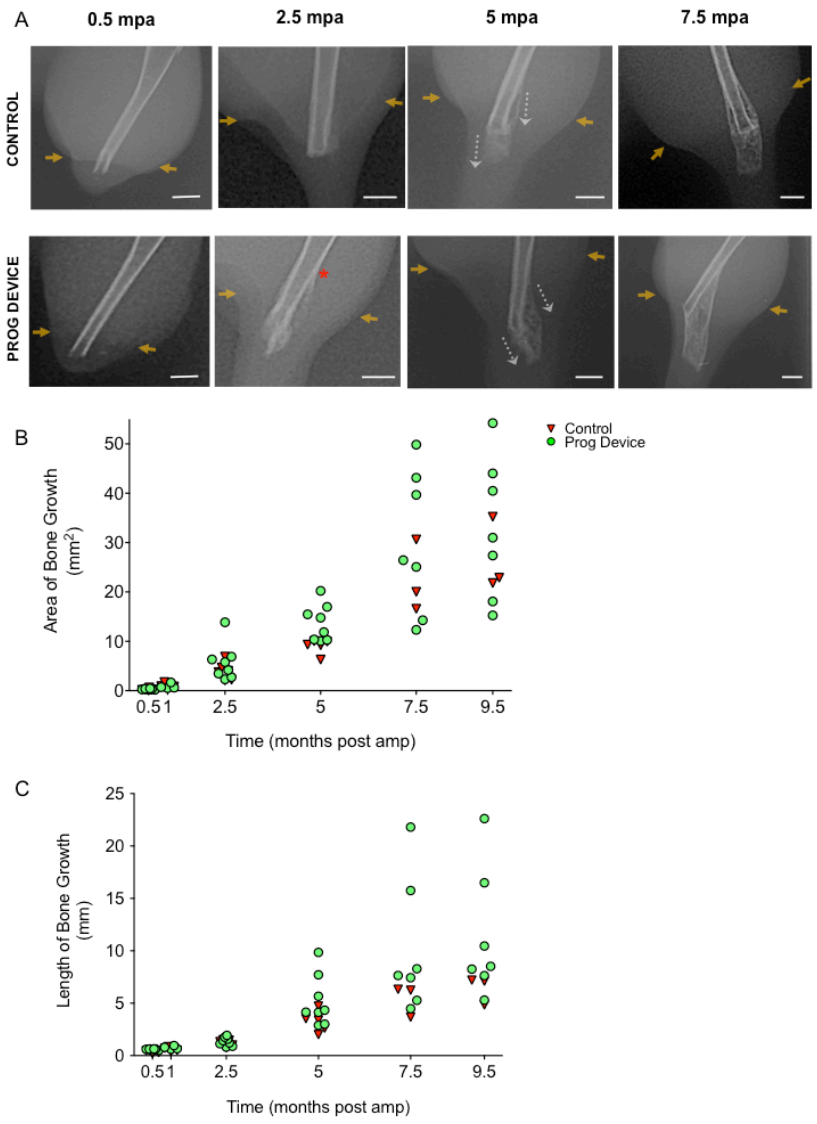

Supplementary Fig. S4. Bone patterning as seen under X-ray images over a 9.5-month regenerative period, Related to Figure 2.

A. The morphometric analysis was performed on regenerates belonging each experimental group, Control (top) and Prog-device (bottom), at five selected times for a 9.5-month period: 0.5, 1, 2.5, 5, 7.5 and 9.5 months post amputation (mpa). The lateral brown arrows indicate amputation plane. As soon as 2.5 mpa, new bone growth above the amputation plane (red asterisk) is detected in treated animals, suggesting that the necessary catalyst for bone regeneration (as it creates more bone resorption and degradation) is enhanced by treatment. **B, C.** Overall, treated animals show a tendency for bigger area (B) and longer (C) new bone growth. As might be expected with the variability of genetic background, individual animals are clearly observed to be strong treatment 'Responders', while other treated animals behaved as 'Non-responders', similar to individuals in Control group. See Supplementary Fig. S2 for details and meaning of the

measurements. Scale bar = 0.5 cm. Values are represented with scatter plots, where each dot represents one animal.

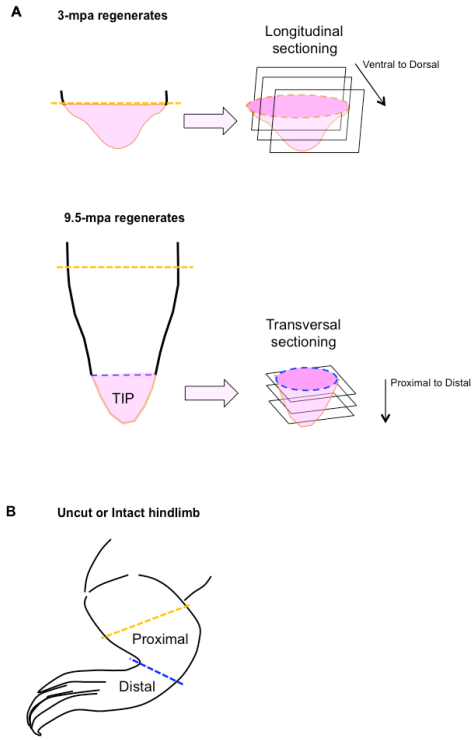

Supplementary Fig. S5. **Experimental design and section axis for histological processing of the regenerates (A) and the uncut or intact frog hindlimb B)**, Related to Figure 1 & Figure 4

A. *Top,* Drawing represent a short-term regenerate, indicating plane for tissue harvesting (orange-dashed line indicates the original amputation site) and longitudinal sectioning, following the ventral-to-dorsal axis. *Bottom,* The most distal portion of the 9.5-mpa regenerates (or tips) were recut approximately 2 cm below the original amputation plane (dashed-blue line indicates plane for recutting and orange-dashed line indicates the original amputation plane). Tips were sectioned along the transversal plane, obtaining cross sections (dashed-blue line) for histological analysis. **B.** Tips of 9.5-mpa regenerates were morphologically compared to the uncut or intact limb. Two different levels of the uncut limb were separately cross-sectioned, immunostained and analyzed: proximal or distal respect to the regular level for the amputation plane (orange-dashed line).

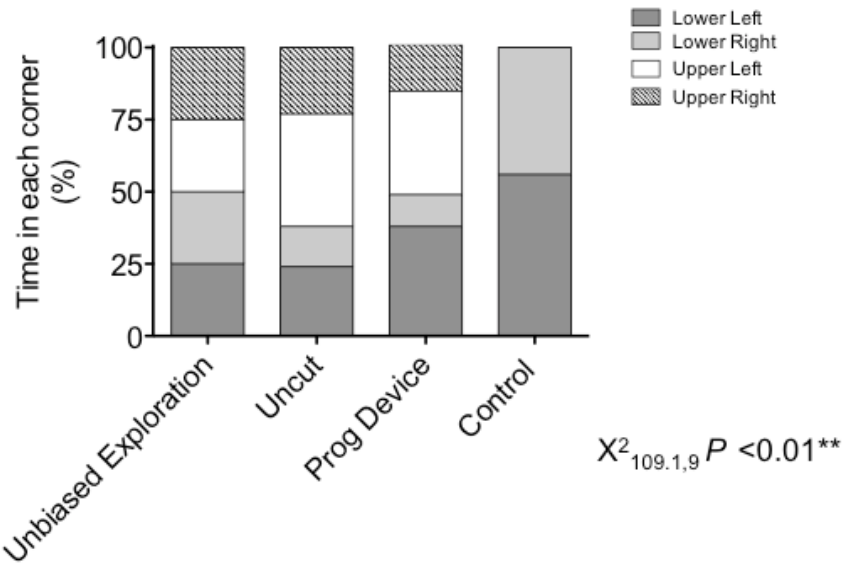

Supplementary Fig. S6. Behavioral observations of exploration and positional information, Related to Figure 5. Contingency analysis for the mean percentage of time spent in each quadrant per experimental group. P <0.01 for $X^2_{(0.05, 9)}$=109.1.

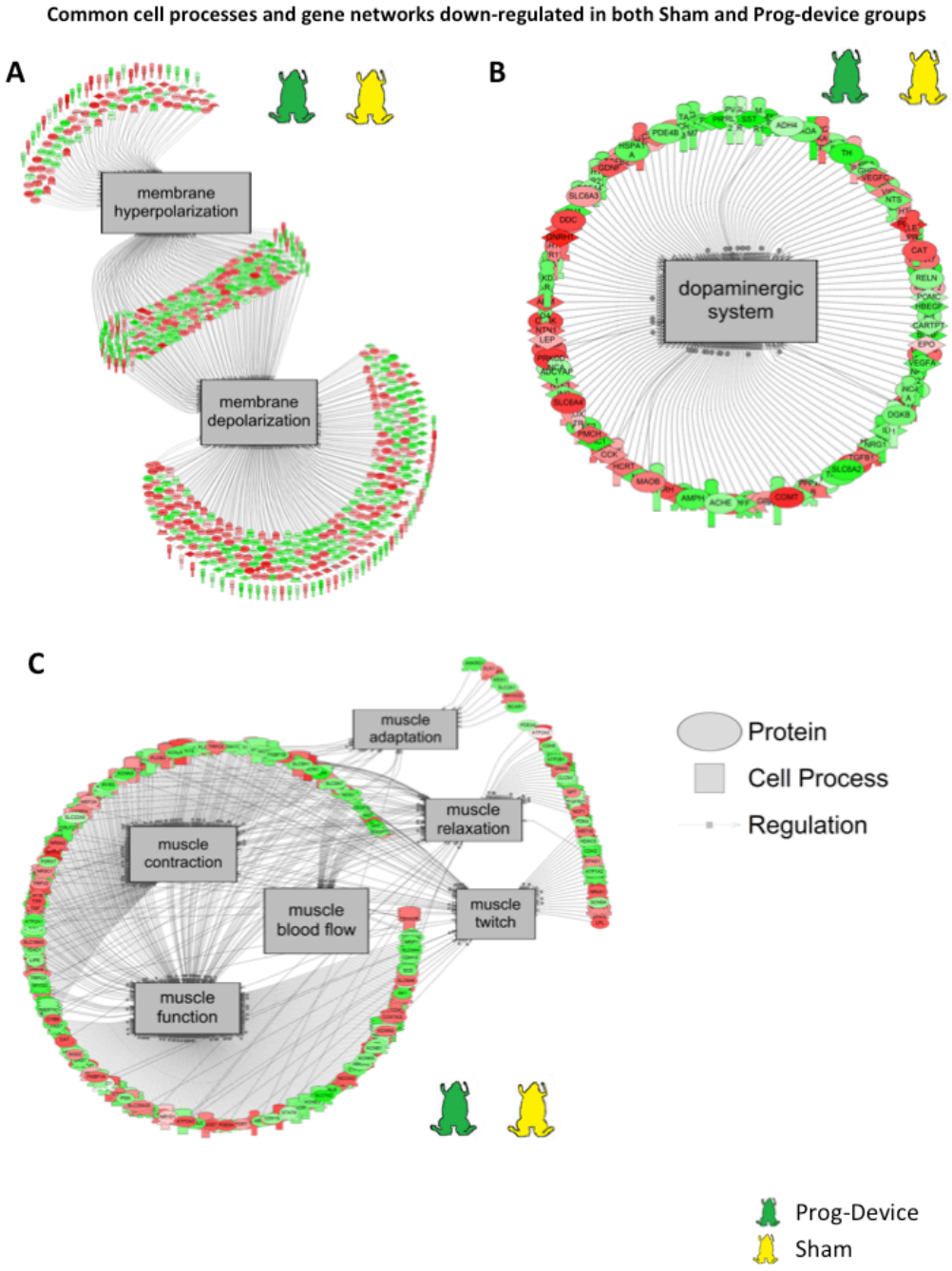

Supplementary Fig. S7. Common down-regulated cell processes and gene networks for both Sham and Prog-device treatments. Related to Figures 6 & 7. Subnetwork enrichment analysis of blastema exposed to only hydrogel device (Sham group) or combined hydrogel plus drug (Prog-Device group) identified common down-regulated pathways involved in (A) changes in membrane potential, (B) dopaminergic system and (C) muscle physiology. Complete data are presented in Appendix 1. All genes within a pathway are located in Appendix 2. Green = down gene, Red = up gene.

Supplementary Table 1. Summary of parameters and variables used to analyze and quantify the regenerated pattern of adult *Xenopus* hindlimb after amputation, Related to STAR Methods.

Abbreviation	Measurement	Analysis details	Formula	Figure
WID	Percentage of width change	Percentage decrease between the width at the base of the regenerate (W_2) and the width at amputation plane (W_1).	$(W_2-W_1)*100/W_1$	Fig. 2A, 2B & Suppl. Fig. S2A
UNA	Unpigmented Area	Percentage of the total regenerated area that is covered by unpigmented skin	pigmented area/ (pigmented + unpigmented area)*100	Fig. 2A, 2B & Suppl. Fig. S2A
LEN	Maximal length of the regenerate (normalized to the total animal length or TOT LEN)	Distance from the amputation plane to the plane set by the tip of the regenerate	LEN/TOT LEN	Fig. 2A, 2B & Suppl. Fig. S2A
SHAPE	Shape characterization	Geometric morphometric analysis based on twelve landmarks or points used to define the profile of the shape of the regenerate	MorphoJ software	Fig. 3E
LEN RATIO	Regenerated vs. Uncut Length Ratio	Quantification of regenerated limb length (a' + b'; a' = length from the knee to the amputation plane, b' = LEN = length from the amputation plane to the tip) relative to the contralateral uncut limb (a + b; a= tibiofibula length, b= tarsus length)	(a'+b')/(a+b)	Fig. 3G
CURVE at tip	Deviation of the tip of regenerate from the reference middle axis	Curvature is considered *positive* when the four most distal landmarks (9, 12, 5 and 6) are situated on the same lateral plane (right or left) respect to the reference middle axis	Categorical variable (n/a)	Suppl. Fig. S2B
BLEN	Maximal length of bone growth from the amputation plane (either ossified and non-ossified)	Distance from the amputation plane to the plane set by the most distal part of the regenerated cartilage	ImageJ on X-ray image	Suppl. Fig. S3A & Suppl. Fig. 4
BAREA	Maximal area occupied by *new* bone growth (non-ossified)	Maximal surface occupied by new bone, without considering amputation plane as the origin, given that regenerate skeletogenesis starts above the amputation plane	ImageJ on X-ray image	Suppl. Fig. S3A & Suppl. Fig. 4
α	Angle deviation of the new bone growth respect to the remaining old bone	Deviation angle formed under the intersection between the middle line of the new bone growth and the middle line of the remaining bone	ImageJ on X-ray image	Fig. 2 & Suppl. Fig. S3B (Left)

d	Displacement (reorganization) of the remaining bone from the middle line after amputation	Geometric intersection between the middle line of the intact tibiofibula bone and the plane set by the base of the regenerate was taken for evaluating the bone deviation from the longitudinal axis (d=0) to the medial edge of the soft tissue (d= -0.5)	ImageJ on X-ray image	Fig. 2 & Suppl. Fig. S3B (Right)
ADPT	Mechanosensitive adaptation	Presence/absence of response motor to one touch stimulus applied 30 seconds after the first one. Both stimuli are applied with toothless-smooth tip forceps in the same direction and with the same weak pressure	Categorical variable (n/a)	
MOV	Efficient motor activity level	Number of efficient movements per 3-min interval. Only movements implying trajectory displacement (swimming between corners, to the water-air surface, etc) were quantified.	Counting of number of active movements per 3-min video	Fig. 5A
RI	Regeneration Index	The RI is a numerical score designed for evaluating the regenerative capacity of Xenopus hindlimb. RI ranges from 0 (typical hypomorphic spike, low regenerative ability) to 10 (patterned limb-like regenerates, high regenerative ability).	RI= $3*x_1 + 2*x_2 + 2*x_3 + 1*x_4 + 1*x_5 + 1*x_6$	Fig. 3F & Suppl. Tables 1&2

Supplementary Table 2. Regeneration Index (RI) scores for individual animals at 2.5 mpa. Related to STAR Methods and Figure 3.

The RI is a numerical score [calculated by the weighted formula RI= $3*x_1 + 2*x_2 + 2*x_3 + 1*x_4 + 1*x_5 + 1*x_6$] designed for evaluating the regenerative capacity of Xenopus hindlimb. RI ranges from 0 (typical hypomorphic spike, low regenerative ability) to 10 (patterned limb-like regenerates, high regenerative ability). Ctrl: untreated Control; PD: Progesterone-device treated animals

		WID ≤ -50% (x_1)	**UNA ≥ 30% (x_2)**	**MaxWID ≥ W1 (x_3)**	**CURVE at tip (x_4)**	**SecBONE AMP (x_5)**	**ADPT (x_6)**	**RI**
CONTROL	Ctrl1	-65% (0)	22% (0)	No (0)	no (1)	No (0)	No (0)	1
	Ctrl2	-58% (0)	23% (0)	No (0)	Yes (0)	No (0)	Yes (1)	1
	Ctrl3	-55% (0)	23% (0)	No (0)	No (1)	Yes (1)	Yes (1)	3
	Ctrl4	-54% (0)	18% (0)	No (0)	Yes (0)	Yes (1)	No (0)	1
	Ctrl5	-63% (0)	13% (0)	No (0)	No (1)	Yes (1)	Yes (1)	3
	Ctrl6	-55% (0)	21% (0)	No (0)	No (1)	No (0)	No (0)	1
	Ctrl7	-56% (0)	12% (0)	No (0)	yes (0)	No (0)	No (0)	0

PROG DEVICE	PD1	-7% (1)	50% (1)	No (0)	No (1)	No (0)	Yes (1)	7
	PD2	-39% (1)	50% (1)	Yes (1)	No (1)	Yes (1)	Yes (1)	10
	PD3	-61% (0)	34% (1)	No (0)	Yes (0)	Yes (1)	Yes (1)	4
	PD4	-47% (1)	27% (0)	No (0)	No (1)	Yes (1)	No (0)	5
	PD5	-28% (1)	39% (1)	Yes (1)	No (1)	Yes (1)	Yes (1)	10
	PD6	-58% (0)	11% (0)	No (0)	No (1)	No (0)	Yes (1)	2
	PD7	-44% (1)	31% (1)	Yes (1)	No (1)	Yes (1)	Yes (1)	10
	PD8	-27% (1)	41% (1)	Yes (1)	No (1)	Yes (1)	Yes (1)	10
	PD9	-52% (0)	57% (1)	No (0)	No (1)	No (0)	Yes (1)	4

Supplementary Table 3. **Regeneration Index (RI) scores for individual animals at 9.5 mpa.** Related to STAR Methods and Figure 3

The RI is a numerical score [calculated by the weighted formula RI= $3*x_1 + 2*x_2 + 2*x_3 + 1*x_4 + 1*x_5 + 1*x_6$] designed for evaluating the regenerative capacity of Xenopus hindlimb. RI ranges from 0 (typical hypomorphic spike, low regenerative ability) to 10 (patterned limb-like regenerates, high regenerative ability). Ctrl: untreated Control; PD: Progesterone-device treated animals.

		WID ≤ -50% (x_1)	**UNA ≥ 10% (x_2)**	**MaxWID ≥ W1 (x_3)**	**CURVE at tip (x_4)**	**BONE AREA ≥ 30% (x_5)**	**ADPT (x_6)**	**RI**
CONTROL	Ctrl1	-57% (0)	4% (0)	No (0)	Yes (0)	35% (1)	Yes (1)	2
	Ctrl2	-66% (0)	3% (0)	No (0)	No (1)	23% (0)	No (0)	1
	Ctrl3	-62% (0)	4% (0)	No (0)	Yes (0)	22% (0)	No (0)	0
PROG-DEVICE	PD1	-53% (0)	11% (1)	No (0)	No (1)	18% (0)	Yes (1)	4
	PD2	-39% (1)	16% (1)	No (0)	No (1)	41% (1)	Yes (1)	8
	PD3	-64% (0)	8% (0)	no (0)	No (1)	31% (1)	Yes (1)	3
	PD4	-46%	14%	No	No	27%	Yes	7

		(1)	(1)	(0)	(1)	(0)	(1)	
	PD5	-47% (1)	19% (1)	Yes (1)	Yes (1)	44% (1)	Yes (1)	10
	PD6	-49% (1)	8% (0)	No (0)	No (1)	15% (0)	Yes (1)	5
	PD7	-43% (1)	20% (1)	Yes (1)	No (1)	54% (1)	Yes (1)	10

Supplementary Table 4. Quantitative measurements for nerve fibers (Tubulin) and vessels (SMA) on cross sections of 9.5-mpa tips of regenerates for Control (amputated untreated) and Prog-device (amputated treated) vs. Uncut (unamputated) limbs. Related to Figure 4.

Values are presented as mean ± s.d. Values for uncut limb correspond to measurements done on 10 sections of two different animals. Proximal and distal are referred to the distance from the amputation plane level (see Supplementary Fig. S5B for illustration).

	Tubulin			SMA		
	Number/slice	**Area/unit (μm^2)**	**Area occupied (%/slice)**	**Number/slice**	**Area/unit (μm^2)**	**Area occupied (%/slice)**
Control	109 ± 38	351 ± 168	2 ± 1	24 ± 10	451 ± 206	0.4 ± 0
Prog-Device	289 ± 119	972 ± 515	10 ± 3	90 ± 50	695 ± 327	2.2 ± 1.2
Uncut Proximal	88 ± 30	2362 ± 233	8 ± 3	65 ± 13	1160 ± 227	0.5 ± 0.3
Uncut Distal	209 ± 25	1582 ± 155	12 ± 1	92 ± 21	870 ± 120	1.4 ± 0.7

Supplementary Table 5. Raw reads and unique sequences aligned to *Xenopus*, as well as the percentage of uniquely mapped reads for each of the 9 blastema samples. Related to STAR Methods and Figures 6 & 7

Samples	Raw_Reads_Num	Unique_Aligned	Uniquely mapped reads %
D18-3349_Sham 1	4183730	2299797	57.61%
D18-3350_Sham 2	4764212	2661956	58.33%
D18-3351_Sham 3	3989349	2084680	54.91%
D18-3358_Prog 1	5912683	3926416	68.34%
D18-3359_Prog 2	4517872	2471849	57.39%
D18-3360_Prog 3	5125074	3249883	65.64%
D18-3367_No device 1	4682793	2800421	62.77%
D18-3368_No device 2	4076875	2139389	55.44%
D18-3369_No device 3	5446437	3460304	65.74%

Supplementary Table 6. List of differentially expressed genes in blastema of Sham and Progesterone-device treatments, compared to Control group, respectively. Genes depicted are those that show greater than log2 fold change of 4. All differentially expressed genes can be found in Appendix S1. **Related to Figure 7**

Treatment	Gene Name	Gene ID	log2 Fold change	p-value (FDR)
Sham	NADH dehydrogenase [ubiquinone] 1 beta subcomplex subunit 10-like	LOC108718674	-7.24	3.69E-02
	zinc finger protein 850-like	LOC108718435	-7.12	4.37E-02
	enhancer of polycomb homolog 1-like	LOC108719842	-5.92	4.53E-02
	ras related glycolysis inhibitor and calcium channel regulator	rrad	-4.75	1.37E-02
	kelch like family member 34	klhl34	-4.50	1.10E-02
	actin related gene 3	act3	-4.38	5.20E-03
	pancreatic progenitor cell differentiation and proliferation factor-like protein	LOC108719245	-4.23	1.31E-02
	alpha-actinin-3	LOC108715125	-4.21	1.37E-02
	adenylate kinase 1	ak1	-4.20	3.41E-03
	parvalbumin	pvalb	-4.18	3.60E-02
	myozenin 1	myoz1	-4.16	8.84E-03
	RNA binding motif protein 24	rbm24	-4.15	4.32E-02
	troponin C2, fast skeletal type	tnnc2	-4.12	4.57E-02
	ras related glycolysis inhibitor and calcium channel regulator	rrad	-4.08	2.13E-03
	Y-box binding protein 3	ybx3	-4.01	1.37E-02
	SMAD family member 4	smad4	5.63	3.60E-02
	olfactory receptor 51L1-like	LOC108709051	6.39	3.72E-02
	capZ-interacting protein-like	LOC108707388	7.15	7.55E-03
Prog-Device	prolactin	prl	-7.30	4.18E-02
	myosin light chain 4	myl4	-6.91	3.65E-02
	arginine vasopressin	avp	-6.72	2.87E-03
	LBH domain containing 1	lbhd1	-6.52	8.55E-04

	unknown	LOC108701576	-6.43	2.46E-03
	carcinoembryonic antigen-related cell adhesion molecule 19-like	LOC108696713	-6.41	1.71E-03
	ELMO domain containing 1	elmod1	-6.38	1.45E-03
	ryncolin-1-like	LOC108698848	-6.07	2.09E-02
	olfactory receptor family 52 subfamily D member 1	or52d1	-5.98	2.70E-02
	RAS like family 12	rasl12	-5.82	2.02E-02
	unknown	LOC108699555	-5.67	2.26E-02
	carbonic anhydrase 12	ca12	-5.67	1.96E-02
	uncharacterized protein C7orf50 homolog	LOC108701567	-5.67	1.95E-02
	somatostatin	sst	-5.63	2.56E-02
	mannosidase beta like	manbal	-5.61	4.58E-02
	cholinergic receptor nicotinic alpha 7 subunit	chrna7	-5.50	3.55E-02
	kelch like family member 40	klhl40	-5.50	4.63E-06
	CUGBP Elav-like family member 4	celf4	-5.36	4.87E-02
	unknown	LOC108708284	-5.36	4.77E-02
	myozenin 2	myoz2	-5.35	4.60E-02
	solute carrier family 1 member 3	slc1a3	-5.13	9.69E-04
	unknown	LOC108719658	-5.12	8.85E-04
	seizure related 6 homolog like 2	sez6l2	-4.67	9.49E-05
	HEAT repeat-containing protein 3-like	LOC108713990	-4.52	3.81E-03
	CUB and sushi domain-containing protein 3-like	LOC108719756	-4.38	5.93E-04
	phospholipid transfer protein	pltp	-4.27	3.13E-03
	xin actin binding repeat containing 1	xirp1	-4.18	7.37E-03
	cadherin 12	cdh12	-4.05	6.24E-03
	ATPase Na+/K+ transporting subunit alpha 3	atp1a3	-4.00	7.42E-03
	interleukin-8-like	loc100498234	4.04	2.31E-02
	transcriptional regulator ATRX homolog	LOC108711024	4.61	1.39E-02
	transmembrane protein 256	tmem256	5.55	3.53E-02
	poly(U)-specific endoribonuclease-D	loc100497154	5.68	3.40E-02
	protein MGARP-like	LOC108706683	5.69	4.49E-02

	capZ-interacting protein-like	LOC108707388	5.78	3.26E-02
	nuclear pore complex protein Nup214-like	LOC108705544	5.78	1.61E-02
	multiple inositol-polyphosphate phosphatase 1 L homolog	LOC108696047	5.80	4.81E-02
	15 kDa selenoprotein	sep15	6.49	1.99E-03
	superoxide Dismutase 3	sod3	6.53	1.28E-02
	histone H2B 1.2	LOC108705674	6.87	1.25E-02
	unknown	LOC108700612	7.52	5.79E-03